Est. 1984

ORIENTAL JOURNAL OF CHEMISTRY

An International Open Access, Peer Reviewed Research Journal

www.orientjchem.org

ISSN: 0970-020 X
CODEN: OJCHEG
2023, Vol. 39, No.(2):
Pg. 284-289

Synthesis and Design of novel morpholinyl mannich bases for Potential Inhibitory Activity of SARS-CoV-2 Main Protease

MOHAMED R. ELAMIN[1]*, SONDOS ABDULLAH J ALMAHMOUD[1], TAREK A. YOUSEF[1,2] , IBRAHIM K. FARH[3], HAJO IDRISS[4,5] and AMIN OSMAN ELZUPIR[1,5]

[1]Department of Chemistry, College of Science, Imam Mohammad Ibn Saud Islamic University (IMSIU), Riyadh 11623, Saudi Arabia.
[2]Toxic and Narcotic drug, Forensic Medicine Department, Mansoura Laboratory, Medicolegal Organization, Ministry of Justice, P.O. Box 12432, Cairo 11435, Egypt.
[3]Department of Pharmaceutical Sciences, College of Pharmacy, King Saud Bin Abdulaziz University for Health Sciences (KSAU-HS),Riyadh, Saudi Arabia.
[4]Department of Physics, College of Science, Imam Mohammad Ibn Saud Islamic University (IMSIU), Riyadh 11623, Saudi Arabia.
[5]Deanship of Scientific Research, Imam Mohammad Ibn Saud Islamic University (IMSIU), Riyadh 11623, Saudi Arabia.
*Corresponding author E-mail: mrabuzaid@imamu.edu.sa

http://dx.doi.org/10.13005/ojc/390207

(Received: March 02, 2023; Accepted: April 15, 2023)

ABSTRACT

In this study, a new mannich base 1-(2H-1,3-benzodioxol-5-yl)-3-(morpholin-4-yl)propan-1-one (Mor) was successfully prepared in good yield. The structure of the title compound was elucidated by ^{1}H-NMR, FT-IR, UV-Vis and electron-impact mass spectroscopy. The inhibitory activity of Mor against SARS-CoV-2 main protease (M^{pro}) was investigated by means ofmolecular docking approach. Mor showed excellent binding affinity to the active residues of M^{pro} with low binding score energy. Further improvements in the results were obtained by four designated analogues to Mor, characterized by the introduction of different methoxyl and hydroxyl substituents. The hydroxyl groups in Mor analogues significantly improve the binding affinity to the active site of M^{pro} to 56%, the binding energy to -6.3 kcal/mol, as well as the ability to form hydrogen bonds compared with nirmatrelvir as the reference Mpro inhibitor.

Keywords: Morpholine, Docking, Mannich bases, Morpholine, SARS-CoV-main protease.

INTRODUCTION

Modern medicinal chemistry includes research on novel antiviral medicines as one of its top focus areas[1]. Because viral infections are prevalent, and new hazardous viral diseases are developing due to pathogenic strains such as Coronaviruses and influenza viruses[2]. There has

been a severe outbreak of severe acute respiratory syndrome coronavirus 2 (SARS-CoV-2) in China since the end of 2019, prompting a global response and posing a severe threat to public health. Currently, there is a limited treatment for COVID-19, which is caused by severe acute respiratory syndrome coronavirus 2 (SARS-CoV-2). Therefore, identifying potential pharmacological treatments for this disorder is imperative.

Nitrogen-containing heterocycles ((N-heterocycles) received considerable attention due to their significant therapeutic efficacy[4]. Heterocycles containing nitrogen and their synthetic analogs may produce new medications. Due to their interesting biological properties, these elements are widely used in natural or artificial biological processes.[5] These compounds possess a wide variety of chemical structures with anti-inflammatory, anti-cancer and anti-viral properties, low toxicity, and the potential to influence multiple cellular targets.[6] Some N-heterocycles found in plants, have long been used as phytochemical medicines[7]. N-heterocycles are crucial for biochemical reactions. biochemical processes in living cells and their widespread distribution in natural products[8]. The primary ingredients of most enzymes consist of aromatic heterocycles, while the primary ingredients of most coenzymes are non-amino acids[9]. The most important nitrogen-containing heterocyclic compounds have numerous biological targets with their structural and pharmacological properties[10].

Among many N-containing heterocycles, morpholine derivatives have attracted considerable attention due to their biological actions, which can be found in various therapeutic fields.

Morpholines can be considered a fundamental class and essential component in chemical synthesis, and many morpholine derivatives have attracted attention due to their unique and diverse uses. It is frequently chosen as a precursor material for synthesizing enantiomerically pure-amino acids, -amino alcohols, and peptides[12]. The popularity of the morpholine moiety can be attributed to many reasons. For instance, the oxygen atom at the center of morpholine might participate in donor-acceptor-type interactions with the appropriate receptor, increasing binding affinity. Moreover, the electronegative effect of oxygen atom's decreases the nitrogen atom's basicity[13]. In addition, morpholine derivatives are one of the structural components of many natural sources,[14], such as alkaloids, polygonapholine, chelonian, antioxidant and chelonian[15,16].

Chelonian showed antibacterial action against *Bacillus subtilis* and an anti-inflammatory impact, whereas the two novel spiro alkaloids demonstrated antioxidant characteristics[17]. Due to the aforementioned biological aspects of morpholine, the current study aims to synthesize new morpholinyl mannich base and investigate their capability to inhibit the main protease of SARS-CoV-2 via molecular docking studies.

MATERIALS AND METHODS

Synthesis of 1-(2H-1,3-benzodioxol-5-yl)-3-(morpholin-4-yl)propan-1-one (Mor)

Morpholine (1.74 mL, 2.00 mmol), paraformaldehyde (612 mg, 2.00 mmol) and hydrochloric acid (few drops) were dissolved in dimethyl sulfoxide (40 mL) and the mixture was stirred at 100°C for 12 hours. Then 3,4-(methylenedioxy) acetophenone (3.35 g, 2.00 mmol) was added to the mixture, and the pH was adjusted to around 2-3. The reaction was monitored by RP-HPLC-UV to completeness. The reaction mixture was allowed to cool to room temperature, neutralized to pH 7 using concentrated NaOH, then poured into distilled water (60 mL). The formed greyish yellow precipitate was collected by filtration, washed with acetonitrile, and left to dry in air to give the title compound (yield 78 %). ^{1}H NMR (500 MHz, $CDCl_3$) 7.56 (dd, *J*=8.2, 1.7 Hz, 1H), 7.43 (d, *J*=1.7 Hz, 1H), 6.85 (d, *J*=8.2 Hz, 1H), 6.05 (s, 2H), 3.71 (t, *J*=5.0 Hz, 2H), 3.10 (t, *J*=5.0 Hz, 2H), 2.81 (t, *J*=5.0 Hz, 4H), 2.53–2.48 (m, 4H). FT-IR: 2895, 2801, 1661, 1588, 1422,1250, 1217, 1013 cm^{-1}; EI-MS m/z $[M-H]^+$ 262 (requires for 263.1158 $C_{14}H_{17}NO_4$).

Molecular docking

The ligands were prepared using ChemSketch in mol forms. Then converted to PDB forms with OpenBabel online tools converter, enabling add hydrogens and generate 3D coordinates functions. The reference, Nirmatrelvir, used in this study, and was obtained from PubChem library. Their structures energies were minimized utilizing the Molecular Modeling Toolkit plugin UCSF Chimera

software, attempting 5000 steepest descent steps of 0.02 Å and 5000 conjugate gradient steps of 0.02 Å. The charges were assigned using antechamber. The crystal structure of the 3D Mpro was taken from the Protein Data Bank (PDB ID: 6Y2E). In order to prepare it for docking analysis, water residues have been removed, the missed hydrogens were added, and net charge was computed using antechamber[36]. Then its energy was minimized using the same tools and protocols used for ligands, utilizing 1000 steepest descent steps and 20 conjugate gradient steps. Molecular docking was achieved out with AutoDock Vina plugin UCSF Chimera software. The grid box size used was (32.0, 61.0, 60.0) Å, centered at (–17.0×-25.0×16.0) Å. Conformers images interaction with the active sites of M^{pro} of SARS-CoV-2 were visualized and processed via UCSF Chimera software[18-24].

RESULTS AND DISCUSSION

Synthesis and characterization

The target compound (MOR) was synthesized using a reported procedure and the synthetic route is illustrated in Scheme 1. Compound MOR was synthesized be dissolving morpholine and paraformaldehyde in DMSO and after adjusting the PH of the solution to around 2-3, acetophenone derivative was added and the target compound was obtained in a good yield.

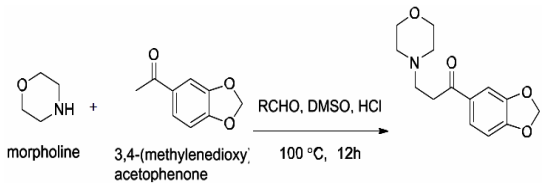

Scheme 1. Synthetics route of Mor

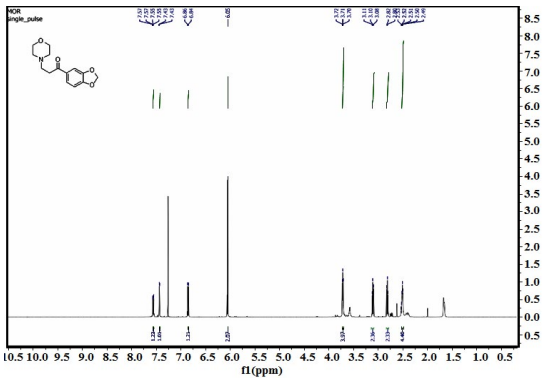

Fig. 1. ^{1}H-NMR spectra of Mor

The structure of the final compound was characterized by ^{1}H-NMR, FT-IR and mass spectroscopy. In ^{1}H-NMR (Fig. 1), the disappearance of the singlet peak around 2.53ppm which corresponds to the CH_3 group in the starting materials material (3,4-(Methylenedioxy) acetophenone)[25] along with the appearance of the triplet peak at 3.71 ppm indicate a successful coupling. FT-IR spectrum (Fig. 2.) did not show any signs of the presence of NH stretch bands in the range 3310-3350 cm^{-1} which indicates the formation of C-N bond. The UV-Vis absorption spectrum of MOR is presented in Fig. 3, and was carried out in methanol solution (2ppm). The UV-Vis absorption spectrum of MOR shows a wide absorption band in the UV region from 200nm to 400nm with four maxima of absorption (λ_{max}) at 237, 262, 309 and 315nm. Fig. 4 showed the mass spectra of MOR using electron impact technique. The present of the parent molecular peak with the mass of 262 for m/z $[M-H]^+$ was detected.

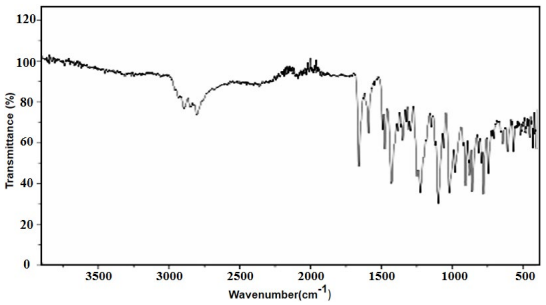

Fig. 2. FT-IR spectra of Mor

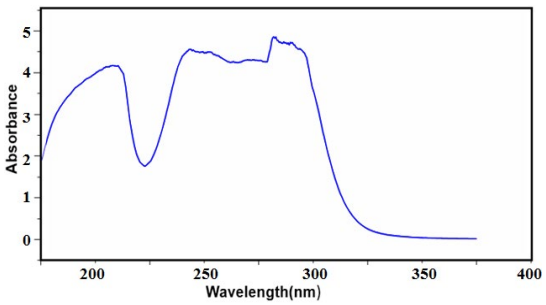

Fig. 3. Absorption spectra of Mor (2ppm)

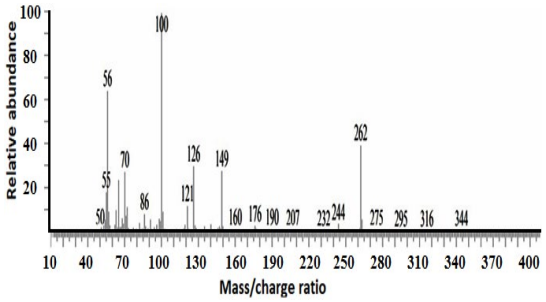

Fig. 4. Mass spectra of Mor

Dockinganalysis

MOR ligand was docked to the active site of M^{pro} with promising binding energy ranged from-5.5 to -5.9 kcal/mol. The lower bound RMSD is 0.00 and upper bound is 6.96, indicating stable and good binding affinity to M^{pro} receptor. The binding affinity or the preferences of the conformers to be docked to the active site was 44%. To test the efficiency of the docking investigation, Nirmatrelvir was docked to the M^{pro} as a reference. Nirmatrelvir was thoroughly studied as M^{pro} inhibitor[25-27]. Its shows binding affinity of 11% to the active pocket, with binding energy of 6.5 kcal/mol and RMSD ranged from 22.535 to 26.1. Nirmatrelvir do not show a hydrogen bond to GLU 166 residue as well as catalytic dyad of HIS 41 and CYS 145, its form hydrogen bond to CYS 44 (Figure 5).

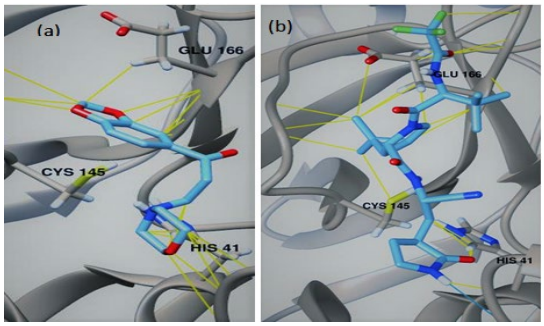

(a) (b)

Fig. 5. (a) Mor in complex form with SARS-CoV-2 main protease with particular attention to the active residues of GLU 166, CYS 145, HIS 41. (b) The reference of Nirmatrelvir/M^{pro} complexes. Nitrogen atoms of ligands are blue, oxygens are red, and hydrocarbons are cyan. Blue lines represent hydrogen bonds, and yellow represent van der Waals forces

To further improve these results four compounds were designed, introducing the different substituents to phenyl group (Scheme 2). The full results were listed in Table 1. The replacement of methoxy groups with hydroxyl groups significantly improve the efficiency of the docking by increasing the binding affinity to the active site of M^{pro}, score energy, as well as the ability to form hydrogen bonds (Figure 6).

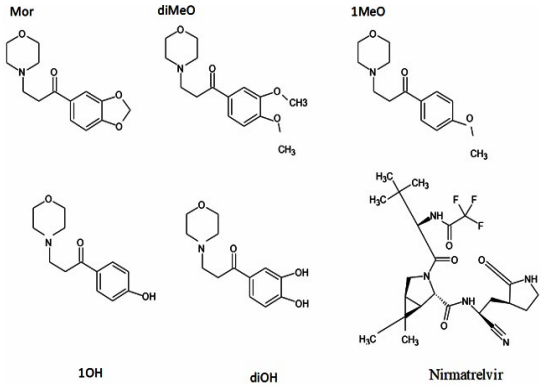

Scheme. 2. Chemical structures of synthesized MOR, its designed analogues, and the reference compound nirmatrelvir

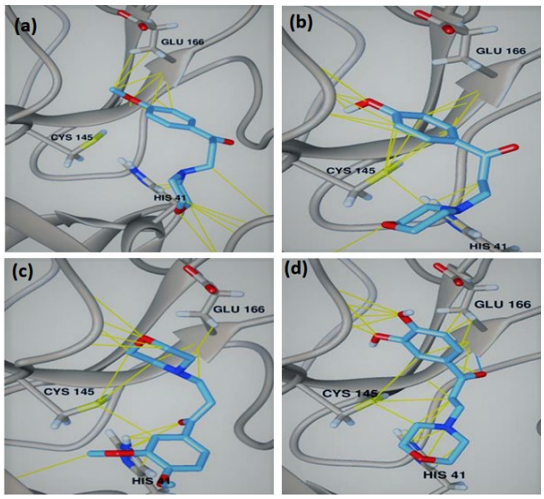

Fig. 6. (a) 1MeO in complex form with SARS-CoV-2 main protease with particular attention to the active residues of GLU 166, CYS 145, HIS 41. (b) 1OH/M^{pro} complexes. (c) diMeO/M^{pro} complexes. (d) diOH/M^{pro} complexes. Nitrogen atoms of ligands are blue, oxygens are red, and hydrocarbons are cyan. Blue lines represent hydrogen bonds, and yellow represent van der Waals forces

All ligands and nirmatrelvir reference were interacted to the catalytic dyed of HIS 41 and CYS 145 via van der Waals forces. The compound diOH show high ability to form hydrogen bonds with several residues including CYS 145 and GLU 166, with RMSD significantly higher than that reported for nirmatrelvir, and comparable binding score energy up to 6.3 kcal/mol. The carbonyl group in diOH form hydrogen bond to the important residue GLU 166 with a distance of 2.195 Å. Further, the binding affinity to the M^{pro} active site is 56%.

Table 1: The binding affinities the synthesized Mor, its designed analogues, and the reference compound nirmatrelvir with main protease of SARS-CoV-2 (M^{pro})

ID	Binding affinity	Score Kcal/mol	RMSD	Hydrogen bonding	van der Waals
Mor	44%	-5.5 to -5.9	0.0 to 6.96	-	HIS163, MET49, HIS41, SER46, GLU166, THR45, ASN142, THR25, CYS145, THR24, CYS44, PHE140, MET165, LEU141, HIS164
diOH	56%	-5.5 to -6.3	0.0 to 5.99	CYS145, HIS163, GLU166, LEU141, SER144, PHE140	LEU141, HIS163, PHE140, GLU166, SER144, MET 165, MET 49, CYS145, ASN142, HIS41, HIS164, GLY143, THR25, LEU27
diMeO	11%	-5.4	27.28 to 31.81	-	MET49, THR25, LEU27, GLU166, HIS163, HIS41, ASN142, LEU141, CYS145, SER144, PHE140
1OH	44%	-5.4 to -5.5		HIS163, GLU166, LEU 141	SER144, ASN142, LEU141, PHE140, HIS163, GLU 166, MET 165, THR 25, HIS 41, CYS 44, CYS 145, HIS41, THR25
1MeO	11%	-5.5	28.87 to 31.28	-	MET165, GLU166, HIS163, CYS44, MET165, CYS145, MET49, THR25, SER46, GLN189, THR45, HIS

CONCLUSION

In conclusion, this work presents the synthesis of the ligand Mor, which was successfully synthesized and characterized by FT-IR, NMR, and EI-MS, and UV-Vis. Analogous ligands with methoxy and hydroxy groups were designed and their activity against Mpro was investigated by means of molecular docking approach. The designed and synthesized ligands showed excellent binding affinity to the active residues of M^{pro} with low binding energy. Our results suggest that these ligands may be potential candidates for SARS-CoV-2 M^{pro}, especially the compound diOH, and thus further studies *In vitro* and I*n vivo* are recommended.

ACKNOWLEDGMENT

This research was supported by the Deanship of Scientific Research, Imam Mohammad Ibn Saud Islamic University (IMSIU), Saudi Arabia, Grant No. (21-13-18-046).

Conflicts of interest

The authors declare no conflict of interest.

REFERENCES

1. Wang Z.; Cherukupalli S.; Xie M.; Wang W.; Jiang X.; Jia R, Pannecouque C.; De Clercq E.; Kang D.; Zhan P.; Liu X. *J. Med. Chem.*, **2022**, *17*;*65*(5), 3729-57.
2. Pantaleo G.; Correia B.; Fenwick C.; Joo VS.; Perez L. *Nat. Rev. Drug Discovery.*, **2022,** *21*(9), 676-96.
3. Li CX.; Noreen S.; Zhang LX.; Saeed M.; Wu PF.; Ijaz M.; Dai DF.; Maqbool I.; Madni A, Akram F.; Naveed M., *Biomed. Pharmacother.*, **2022,** 1, 146, 112550.
4. Jiang J.; An Z.; Li M.; Huo Y.; Zhou Y.; Xie J.; He M. *J. Environ. Chem. Eng.*, **2023,** *1*;*11*(1), 109193.
5. Aatif M.; Raza MA.; Javed K.; Nashre-ul-Islam SM.; Farhan M.; Alam MW., *Antibiotics.*, **2022,** *11*(12), 1750.
6. Łowicki D.; Przybylski P. *Eur. J. Med. Chem.*, **2022**, *18*, 114303.
7. Gao B.; Yang B.; Feng X.; Li C., *Nat. Prod. Rep.*, **2022**, *39*(1), 139-62.
8. Insuasty D.; Castillo J.; Becerra D.; Rojas H.; Abonia R., *Molecules.*, **2020**, *24*, *25*(3), 505.
9. Minhas R.; Bansal Y.; Bansal G., *Med. Res. Rev.*, **2020**, *40*(3), 823-55.
10. Kerru N.; Gummidi L.; Maddila S.; Gangu KK.;Jonnalagadda SB., *Molecules.*, **2020**, *20*;*25*(8), 1909.
11. Gattu R.; Ramesh SS.; Nadigar S.; Ramesh S., *Antibiotics.*, **2023,** *7*;*12*(3), 532.
12. Chen C.; Guo SM.; Sun Y.; Li H.; Hu N.; Yao K.; Ni H.; Xia Z.; Xu B.; Xie X.; Long YQ., *Eur. J. Med. Chem.*, **2023,** *11*, 115267.
13. S.M. Yang.; R. Malaviya.; L. J. Wilson.; R. Argentieri.; X. Chen.; C. Yang.; B. Wang.; D. Cavender.; W. V. Murray., *Bioorg. Med. Chem. Lett.*, **2007**, *17*, 326.
14. Wei JS.; Yang S.; Wei Y.; Shamsaddinimotlagh S.; Tavakol H.; Shi M., *Org. Chem. Front.*, **2023**.

15. L. Yurtta.; Z. A. Kaplancıkl.; Y. Özkay., *J. Enz. Inhib. Med. Chem*., **2013**, *5*, 1040.
16. H. Zhao.; H. Thurkauf.; K. Hodgetts.; X. Zhang., *Bioorg. Med. Chem. Lett*., **2002**, *10*, 310.
17. M. Kimura.; T. Masuda.; K. Yamada.; N. Kubota.; N. Kawakatsu.; M. Mitani.; K. Kishii.; M. Inazu.; T. Namiki., *Bioorg. Med. Chem. Lett*., **2002**, *12*, 1947.
18. Wang, J.; Wang, W.; Kollman, P. A.; Case, D. A., Automatic atom type and bond type perception in molecular mechanical calculations., *J. Mol. Graph. Model*., **2006**, *25*(2), 247-260.
19. Pettersen, E. F.; Goddard, T. D.; Huang, C. C.; Couch, G. S.; Greenblatt, D. M.; Meng, E. C.; Ferrin, T. E., UCSF Chimera-a visualization system for exploratory research and analysis., *J. Comput. Chem*., **2004**, *25*(13), 1605-1612.
20. Elzupir, A. O. *J. Mol. Struct*., **2020**, *1222*, 128878.
21. Al-Janabi, A. S.; Elzupir, A. O.; Yousef, T. A. *J. Mol. Struct*., **2021**, *1228*, 129454.
22. O'Boyle, N. M.; Banck, M.; James, C. A.; Morley, C.; Vandermeersch, T.; Hutchison, G. R., *J. Cheminformatics*., **2011**, *3*(1), 1-14.
23. Shapovalov, M. V.; Dunbrack Jr, R. L., *Structure.,* **2011**, *19*(6), 844-858.
24. Trott, O.; Olson, A. J. *J. Comput. Chem*., **2010**, *31*(2), 455-461.
25. Umesha B.; and Basavaraju Y. B., *Medicinal Chemistry Research*., **2014**, *23*, 3744-3751.
26. Joyce, R. P.; Hu, V. W., & Wang., *J. Med. Chem. Res*., **2022**, *31*(10), 1637-1646.
27. Chia, C. B., & See, Y. Y., *Med. Chem. Res*., **2022**, *13*(9), 1388-1389.
28. Mótyán, J. A.; Mahdi, M.; Hoffka, G., & T zsér., *J. Int. J. Mol. Sci*., **2022**, *23*(7), 3507.